Short communication

Clay as a dispersant in the catalyst layer for zinc–air fuel cells

Wen-Kai Chao [a], Chih-Ming Lee [a], Shu-Yi Shieu [a], Chih-Cheng Chou [b], Fuh-Sheng Shieu [a],*

[a] Department of Materials Science and Engineering, National Chung Hsing University, Taichung 40227, Taiwan
[b] Department of Chemical Engineering, National Chung Hsing University, Taichung 40227, Taiwan

Abstract

This study proposes a four-layer membrane electrode assembly (MEA) consisting of air-electrode, proton exchange membrane, Zn-electrode with KOH or NaCl aqueous electrolyte and a steel supporter, for use in Zn–air fuel cells. Montmorillonite clay was used to disperse carbon black (CB) and MnO_2 catalyst to improve the performance of the air-electrode. The microstructures of the air-electrode and cell characteristics were investigated by field emission scanning electron microscopy (FE-SEM), optical microscopy (OM) and an electrochemical analyzer. The experimental results indicate that the four-layer MEA for Zn–air fuel cells reached a power density of $6 \, mW \, cm^{-2}$ (at $10 \, mA \, cm^{-2}$) without electrolyte leakage from the cells. The open circuit voltage (OCV) and current density were improved by adding clay to the air-electrode as clay can minimize CB aggregation. In the polarization test, the OCV value (1.40 V) reached approximately 90% of the standard potential (1.65 V) and remained steadily over 48 h. These experimental results demonstrate the four-layer MEA can replace conventional Zn–air fuel cells that utilize aqueous electrolyte.
© 2007 Elsevier B.V. All rights reserved.

Keywords: Membrane electrode assembly; Zinc–air fuel cells; Carbon block; Clay

1. Introduction

Electrolyte and electrodes are the key components of Zn–air fuel cells. One of the major problems in conventional Zn–air fuel cells is the electrolyte leakage, which uses liquid electrolytes. Recently, gel electrolytes have been utilized in Zn–air fuel cells to replace liquid electrolytes such as potassium hydroxide (KOH) [1,2]. The conductivity of gel electrolytes, e.g. KOH with granular hydroponics gel, is very close to that of liquid electrolytes, both of which are greater than $10^{-3} \, S \, cm^{-1}$. The advantage of using gel electrolytes is to avoid electrolyte leakage and extends the lifetime of Zn–air fuel cells. The current trend of design in fuel cells is toward lighter, thinner and smaller structures; in contrast, to the conventional Zn–air fuel cells that have large volumes (thickness 30.0 mm) and occupy a lot of space.

In recent years, Nafion®, a proton exchange electrolyte material, has been widely utilized in various fuel cell applications such as proton exchange membrane fuel cell (PEMFC) [3,4]

and direct methanol fuel cell (DMFC) [5,6]. Nafion® produced by DuPont® is a commonly used membrane for different applications. It relies on liquid water humidification of the membrane to transport protons. The molecular structure of Nafion® copolymer and polymerized perflurosulfonic acid is characterized by a hydrophobic polytetrafluoroethylene (PTFE) backbone and regularly spaced perfluorovinyl ether side-chains, each terminated by a strongly hydrophilic sulfonate ionic group [7]. The conductivity of Nafion® is approximately $2 \times 10^{-4} \, S \, cm^{-1}$ (25 °C, RH = 50%). This study utilizes Nafion® as a barrier layer in conjunction with an aqueous electrolyte in the Zn anode to solve the problem of liquid electrolyte leakage from Zn–air fuel cells.

The characteristics of the air-electrode controls cell efficiency and reliability. In a previous work [8], we reported that inorganic clays could effectively disperse carbon black (CB) particles in water without use of any organic dispersant. The clay dispersion approach is very likely to be utilized in the catalytic support of Zn–air fuel cells to improve their performance as a result of the well-dispersed CB. Based on this technology, a novel four-layer membrane electrode assembly (MEA) was fabricated for use in alkaline zinc–air fuel cells, using clay as a dispersant to disperse carbon black and the MnO_2 catalyst to improve the air-electrode performance.
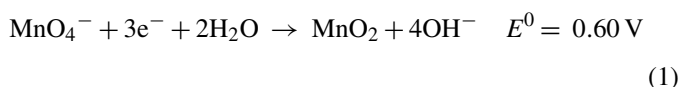
2. Experimental

2.1. Preparation of air-electrodes

Carbon black (Vulcan® XC-72, Cabot) and sodium montmorillonite clay (MMT, Nancor) were used to prepare the catalytic support. The experimental procedures for pulverizing the two powder materials are described below. Both carbon black and clay powders in the designated CB/clay weight ratios of 85/15 and 100/0 were first physically mixed with the ethanol/water (50 g/50 g) co-solvent. Thereafter, the mixture was agitated by stirring for 30 min, and then subjected to an ultrasonic treatment for further agitation at 30–40 °C for another 36 h until completely swollen. Starting with the finely dispersed CB particles, $KMnO_4$ precursor was added to form $CB/clay/KMnO_4$ composites. $KMnO_4$ is a black-purple crystal that can form MnO_2 in neutral or basic solution. The chemical half-reactions of the phase transformation are listed below:

$$MnO_4{}^- + 3e^- + 2H_2O \rightarrow MnO_2 + 4OH^- \quad E^0 = 0.60\,V \tag{1}$$

$$4OH^- \rightarrow 2H_2O + O_2 + 4e^- \quad E^0 = -0.40\,V \tag{2}$$

The composites were dipped in an ethanol solution upon ultrasonic agitation for 36 h before heating to 150 °C for 1 h. After which, the $CB/clay/MnO_2$ hybrid was blended with the PTFE suspension provided by DuPont® with solid content of 60%. It was then subjected to an ultrasonic treatment for another 12 h until completely swollen in ethanol, and dried at 100 °C for 1 h until ethanol and most of the water were completely removed. Finally, the $CB/clay/MnO_2/PTFE$ hybrid was compressed into a membrane to serve as the air-electrode.

2.2. The four-layer membrane electrode assembly

A thin Zn–air fuel cell was fabricated on the basis of a four-layer MEA consisting of Zn-electrode with KOH or NaCl aqueous electrolyte, air-electrode, proton exchange membrane and steel support. First, a Nafion® 117 membrane was cut into 4 cm × 4 cm, and then pretreated with 5 wt% H_2O_2, deionized water, 1.0 M H_2SO_4 and deionized water at 80 °C for 1 h, sequentially. Thereafter, the pretreated Nafion® 117 membrane was sandwiched between Zn-electrode (3 cm × 4 cm × 0.1 cm, 99.98% Strem Chemicals) with 6 M KOH or NaCl aqueous electrolyte and air-electrode. The sandwiched layer was then laid on a steel mesh (4 cm × 8 cm × 0.2 cm, Beam) before fixing by two acrylic plates (8 cm × 4 cm × 0.4 cm). When the Zn-electrode was consumed and oxidized to form ZnO through discharging, it was removed and a new Zn electrode was replaced. The four-layer MEA of the Zn–air fuel cells can be recycled except Zn-electrode. A schematic of the four-layer MEA is shown in Fig. 1. The effective area of the four-layer MEA for a single Zn–air fuel cell was measured to be 9 cm² with the thickness of 0.5 cm.

2.3. Characterization of the air-electrodes and cell performance

The microstructure of electrodes was investigated by field-emission scanning electron microscopy (FE-SEM) (JEOL-6700) and optical microscopy (OM) (Olympus BX51M). Electrochemical characteristics including open circuit voltage (OCV), discharge curves, voltage–current density, and power density–current density of the Zn–air fuel cells were evaluated by an electrochemical analyzer (CHI-614B, CH Instruments). The OCV was measured for the cells stored at an open-circuit condition for 48 h at room temperature (~26 °C).
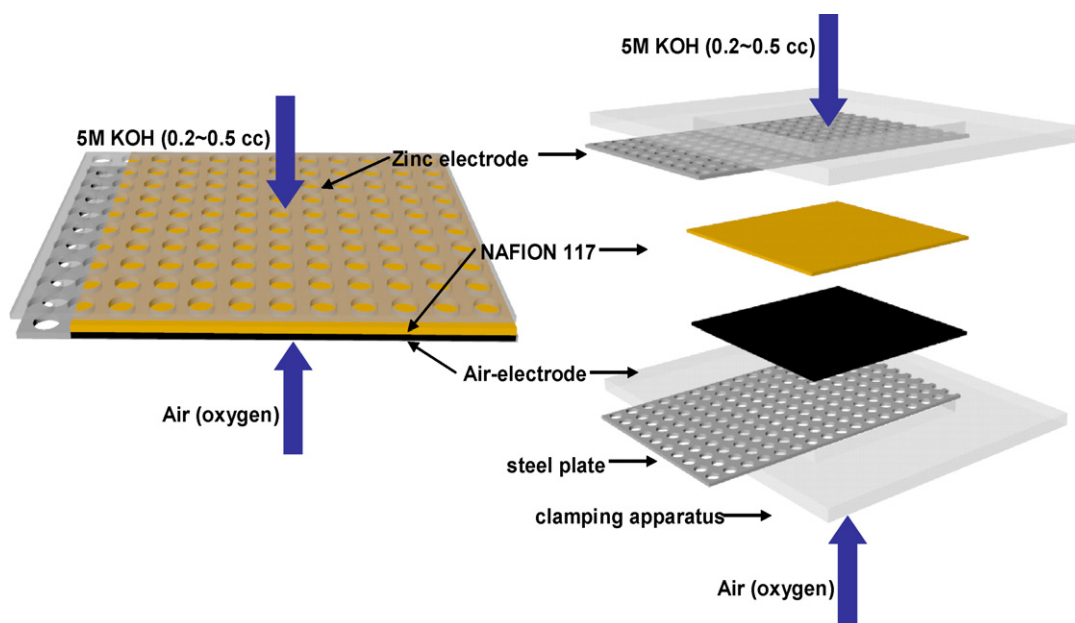

Fig. 1. A schematic of the four-layer membrane electrode assembly.

3. Results and discussion

3.1. Clay as a carbon black dispersant

Carbon black particles were dispersed by adding montmorillonite clay that has unique physical and chemical properties such as high aspect ratios. The microstructure of pristine montmorillonite is irregularly aggregated from a primary unit consisting of aluminosilicate platelets in stacks. The average dimension of each platelet is estimated to be 100 nm × 100 nm × 1 nm [9,10]. The interlayer spacing between neighboring platelets is typically 1.2 nm by XRD measurement [11]. In the clay there is an ionic charge attraction between neighboring platelets, resulting in a face-to-face interaction that forms the primary stack units. van der Waals forces between the platelets cause further aggregation into secondary structures [12]. Due to the strong ionic charges, these clays are capable of swelling in water.

In contrast, CB powder has an aggregated form (>100 nm) with a primary structure of irregular spherical shape and an average diameter of 30–50 nm. Aggregation of the CB particles is caused mainly by van der Waals forces between nanoparticles rather than by ionic charges, as in the case of clay materials [13]. These CB particles are non-dispersible in water and easily form precipitates settled down at the bottom of an aqueous solution. Nevertheless, by subjecting the CB powder to ultrasonic agitation, these powders can be slightly suspended in water, but retain poor swelling capability, and eventually precipitate at the bottom of a container after 24 h. A field-emission scanning electron microscopy (FE-SEM) image, Fig. 2a illustrates the irregular shapes of these pristine CB particles in an aggregated form with an average diameter of 100–1000 nm.

In fact, the settlement of CB can be easily observed at the bottom of aqueous solution by the naked eye, as shown in Fig. 3a and c. By adding clay, the CB/clay hybrid becomes dispersible in co-solvent upon ultrasonic agitation (see Fig. 3b and d). The FE-SEM image in Fig. 2b shows that these CB particles are well dispersed in an aggregated form and have an average diameter of 30–50 nm. To prepare the air-electrode, the CB powder and $KMnO_4$ were suspended in water via clay addition upon ultrasonic agitation, good dispersion of CB/clay hybrids in water is attributable to the presence of swelled montmorillonite clay
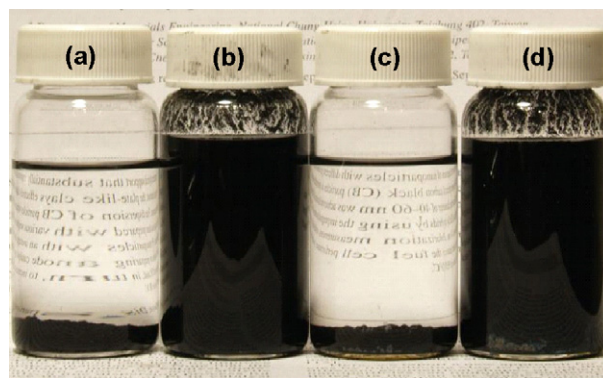

Fig. 3. Photographs of different solutions containing (a) CB, (b) CB/clay, (c) CB/$KMnO_4$ and (d) CB/clay/$KMnO_4$ in water.

in the solvent and its ability to inhibit CB from aggregation. Moreover, XRD analysis indicated that CB/clay hybrids had an 1.2–1.8 nm d spacing, which is similar to that of the pristine clay, implying that the clay platelets retain their original layer-by-layer structure in the primary units. No evidence exists that CB particles undergo an intercalation or are embedded into the clay interlayer. The stacked platelet clay is a steric hindrance to avoid aggregation of the spherical CB particles. Clay facilitates formation of a stable CB dispersion in water because of the hydrophilic characteristic and platelet microstructure.

3.2. Characteristics of the CB/clay/PTFE electrode membrane

An air-electrode is composed of CB, clay dispersant, PTFE suspension and MnO_2 catalyst. The CB powder is primarily responsible for electrical conduction. The clay effectively disperses CB particles and retains the particle size of CB at 50–100 nm. The PTFE suspension, which consists of 60 wt% water and 30 wt% PTFE particles, can bond the CB to the clay, resulting in a conductive membrane once the water is removed. During the catalyst preparation process for air-electrodes, it is noted that the CB powder was completely non-dispersible in water and immediately settled down at the bottom of the beaker due to its hydrophobic characteristic. The surface morphology
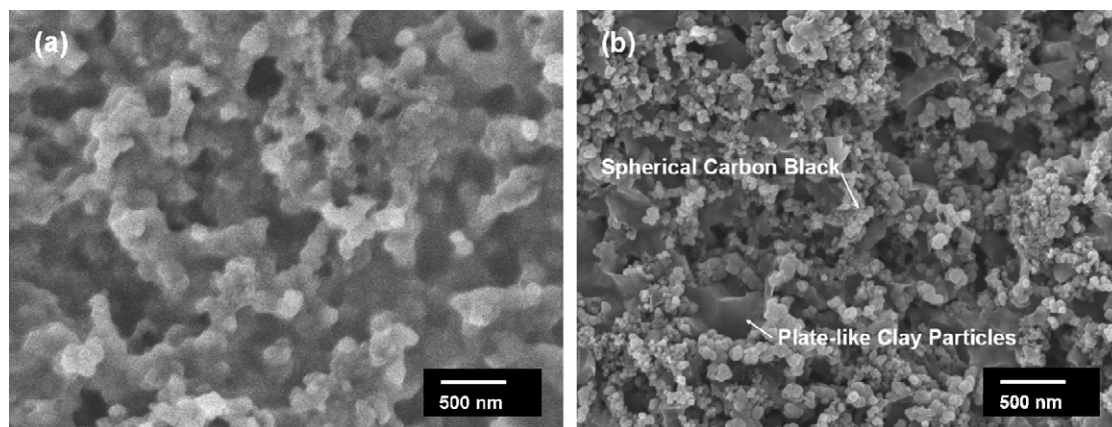

Fig. 2. FE-SEM images of (a) CB powder and (b) CB/MMT/H_2O = 2.50/0.25/97.25 composites.

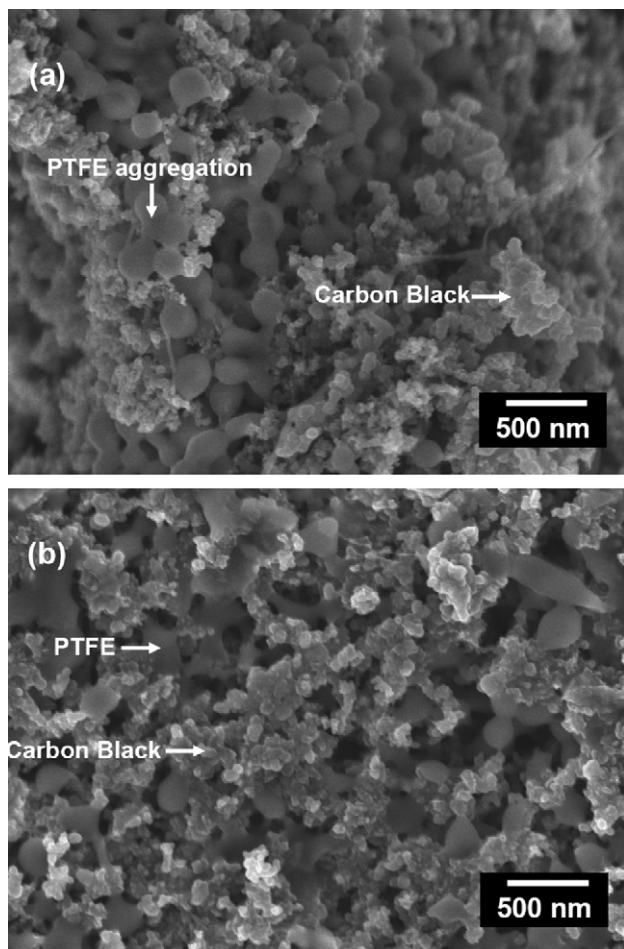Fig. 4. FE-SEM images of (a) CB/PTFE and (b) CB/clay/PTFE membranes.

Fig. 5. *V–I* curves of the air-electrodes in Zn–air fuel cells using (a) KOH and (b) NaCl aqueous electrolytes in the Zn anode.

of air-electrode membranes was analyzed by FE-SEM. The control experiment for the CB/PTFE membrane illustrates that both CB and PTFE powders are in an aggregate form with average diameters of 30–200 and 100–200 nm, respectively, as shown in Fig. 4a. The FE-SEM image in Fig. 4b reveals the microstructure of the CB/clay/PTFE membrane, indicating that CB particles have an average diameter of 30–50 nm and that the adhesive PTFE was well dispersed in the CB matrix.

In an electrical test, the resistance of the CB/clay/PTFE membrane ($40\,\Omega$) was measured to be slightly higher than that of the CB/PTFE membrane ($30\,\Omega$) due to the addition of non-conducting clay. This slight increase in the electrical resistance, however, did not influence the electrochemical performance of the air electrodes as clay addition was only 7 wt%. When clay loading was over 7 wt% in the CB/clay/PTFE membrane, the electrical resistance increased considerably ($\gg 40\,\Omega$), resulted in a decrease in the electrochemical performance of the cell.

3.3. Performance of the membrane electrode assembly

It is known that the structure of an air-electrode that consumes oxygen from the air affects the performance of Zn–air fuel cells directly. In our work, the air-electrode consists of
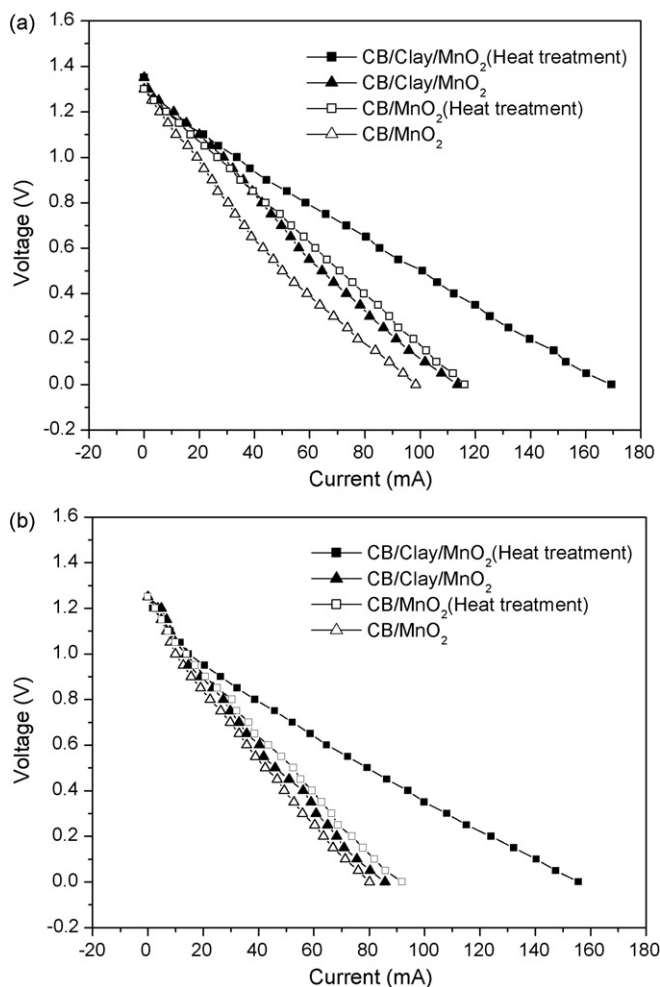
an electrical conductive CB, clay dispersant, PTFE suspension and MnO_2 catalyst. A series of performance tests were conducted for the four-layered MEA by using an electrochemical analyzer instrument. Fig. 5a shows the effect of clay addition in the CB/PTFE membranes with MnO_2 addition on the electrochemical performance of air electrodes in a single cell test. The CB/clay/PTFE membrane with MnO_2 catalyst performed best using KOH electrolyte in the Zn anode, compared with NaCl electrolyte, as shown in Fig. 5b. The four-layer MEA with clay addition achieved the highest short circuit current of 170 mA at 0 V, which is much higher than that without clay addition (120 mA). The conductivity of the Nafion® 117 films is about $2 \times 10^{-4}\,S\,cm^{-1}$ (25 °C, RH = 50%), which is smaller than that of KOH or NaCl aqueous electrolytes because a solid electrolyte has a narrow tunnel that restricts ion exchange and a limited number of proton exchange sites ($-SO_3{}^-$). As a result, the maximum current 170 mA at 0 V of the four-layer MEA in the Zn–air fuel cells is lower than that of a commercial MEA with aqueous electrolyte, 700 mA at 0 V.

In addition, the experimental results indicate that the four-layer MEA in the Zn–air fuel cells avoids electrolyte leakage and achieve a power density of 6 mW cm^{-2} (at 10 mA cm^{-2})
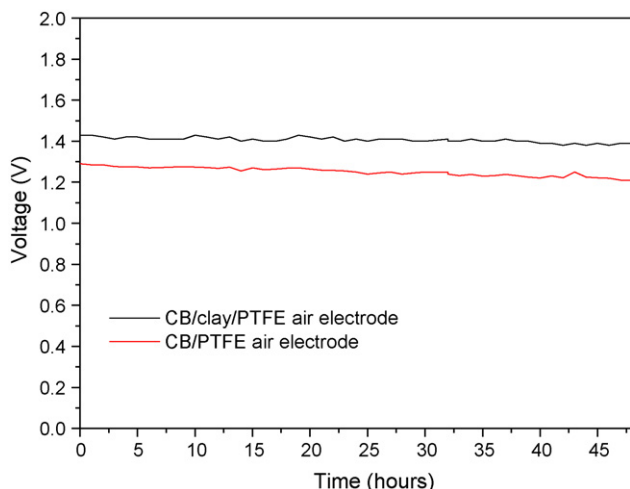
Fig. 6. Open circuit voltage (OCV) measurement of CB/clay/MnO$_2$ and CB/MnO$_2$ PTFE air electrodes for 48 h.

Fig. 7. V–I curves of the air-electrodes using 5 μm catalytic MnO$_2$ with KOH and NaCl electrolytes in the Zn anode.

for the CB/clay/MnO$_2$ with KOH electrolyte. These results evidence that the addition of clay to CB significantly improves the cell performance as the MnO$_2$ catalyst from the KMnO$_4$ precursor was well dispersed in the air electrode. As a result of clay addition, the MnO$_2$ catalyst from the KMnO$_4$ precursor was well-dispersed in the CB/clay/PTFE membrane during the catalytic preparation process. The theoretical potential of a Zn–air fuel cell is 1.65 V at standard condition. The experimental open circuit voltages of the four-layer Zn–air fuel cell, 1.40 V, is lower than the theoretical value, which is very likely due to competing side reactions such as peroxide formation.

Leakage of liquid electrolytes in a Zn–air fuel cell can deteriorate its performance because the electrolyte liquid floods the air-electrode and blocks its oxygen access. The corrosive electrolyte may also damage other components such as the cell case or cell contacts, and block air access holes. In this study the four-layer MEA used only 0.5 ml electrolyte, which was separated from the air-electrode by the Nafion® 117 film to avoid contact between the electrolyte and air-electrode. Fig. 6 presents the long-time performance test in terms of OCV of the CB/clay/PTFE and CB/PTFE membranes in the Zn–air fuel cells. The OCV of the cells remained steady at 1.25 and 1.40 V over 48 h for the CB/MnO$_2$/PTFE and CB/clay/MnO$_2$/PTFE air-electrodes, respectively. In addition to the long-time stability, the four-layer MEA in the Zn–air fuel cell solves the leakage problem.

3.4. Effect of the MnO$_2$ catalyst

The particle sizes of MnO$_2$ can influence the cell performance. To compared with the MnO$_2$ catalyst from the KMnO$_4$ precursor, a commercially available 5 μm MnO$_2$ catalyst was also utilized for the air-electrode. Fig. 7 shows the effect of clay addition in the CB/PTFE membrane with 5 μm MnO$_2$ catalyst. Of the different catalysts, the CB/clay/PTFE membrane in KOH electrolyte performed best, similar to the results using KMnO$_4$ precursor. It is also noted that the cell performance is better in
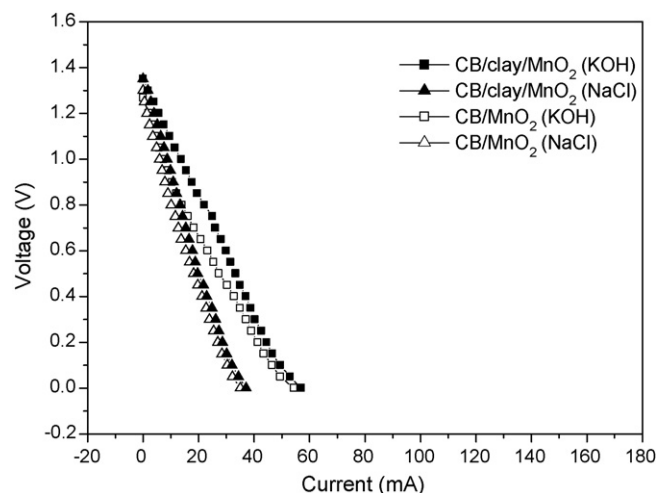
KOH than in NaCl electrolytes. All the cells have an OCV of 1.3–1.4 V, which remains steadily over 48 h.

During the catalyst preparation, a heating treatment at 150 °C transformed the KMnO$_4$ precursor into a MnO$_2$ phase. This method gives good dispersion and small size MnO$_2$ catalyst on the CB support. The particle size of the MnO$_2$ catalyst (∼1 μm), made from the KMnO$_4$ precursor, is smaller than the commercial 5 μm MnO$_2$ catalyst. The air-electrode with MnO$_2$ catalyst made from KMnO$_4$ precursor performed better in terms of current versus voltage than that of the 5 μm MnO$_2$ catalysts due to the insufficient blending between 5 μm MnO$_2$ catalysts and CB particles, as schematically shown in Fig. 8.
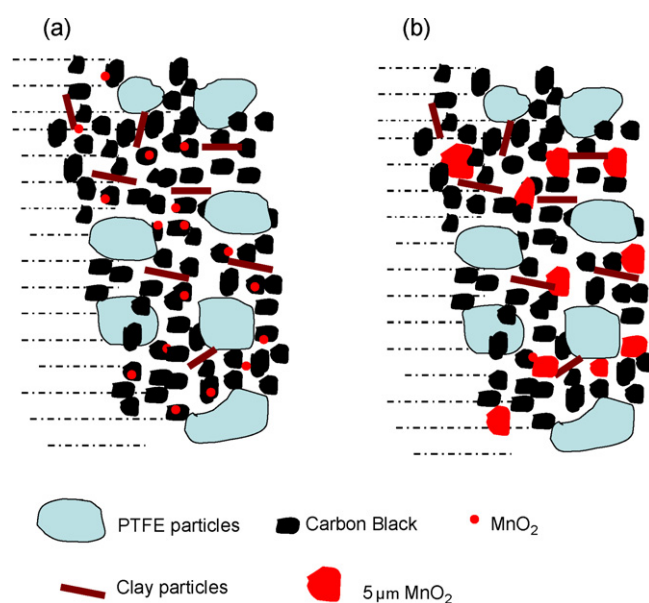

Fig. 8. A graphical illustration of the microstructure in the catalyst layers made of KMnO$_4$ precursor and commercial MnO$_2$ powder. (a) MnO$_2$ (KMnO$_4$) and (b) 5 μm MnO$_2$.

4. Conclusion

This study presents a novel approach of fabricating a four-layer MEA for Zn–air fuel cells that can solve the leakage problem encountered in conventional cells that use liquid electrolytes. By replacing the bulky liquid electrolyte with Nafion® films, the thickness of the four-layered MEA in Zn–air fuel cells was reduced from 30 mm to only 3.0 mm. In preparing the air-electrode, platelet-like montmorillonite clay was utilized to disperse CB and the MnO_2 catalyst along with PTFE as an adhesive. The experimental results indicate that adding clay significantly improves the cell performance in terms of open circuit voltage, voltage–current density characteristics and long-time stability.

Acknowledgements

References

[1] A.A. Mohamad, J. Power Sources 159 (2006) 752.
[2] S. Chandra, S.S. Sekhon, R. Srivastava, N. Arora, Solid State Ionics 154/155 (2002) 609.
[3] S. Lister, G. Mclean, J. Power Sources 130 (2004) 61.
[4] P. Yu, M. Pemberton, P. Plasse, J. Power Sources 144 (2005) 11.
[5] Z.G. Shao, W.F. Lin, F. Zhu, P.A. Christensen, M. Li, H. Zhang, Electrochem. Commun. 8 (2006) 5.
[6] G.Q. Lu, C.Y. Wang, J. Power Sources 134 (2004) 61.
[7] C.K. Wong, Fuel Cell, Chichester Wildfowlers Association, Taiwan, 2003, pp. 4–5.
[8] Y.H. Pai, J.H. Ke, C.C. Chou, J.J. Lin, J.M. Zen, F.S. Shieu, J. Power Sources 163 (2006) 398.
[9] M. Alexandre, P. Dubois, Mater. Sci. Eng. 28 (2000) 1.
[10] J.J. Lin, Y.M. Chen, Langmuir 20 (2004) 4261.
[11] M. Zanetti, S. Lomakina, G. Camino, Macromol. Mater. Eng. 279 (2000) 1.
[12] B.K.G. Theng, Chemistry of Clay–Organic Reactions, Wiley, New York, 1974.
[13] J.N. Israelachvili, Intermolecular & Surface Forces, Harcourt Brace, New York, 2002.